Minimal Energy Transfer of Solid Material Between Planetary Systems

Edward Belbruno[a], Amaya Moro-Martín[a] and Renu Malhotra[b]

[a] Department of Astrophysical Sciences, Princeton University.
[b] Department of Planetary Sciences, University of Arizona.

belbruno@princeton.edu, amaya@astro.princeton.edu, renu@lpl.arizona.edu

ABSTRACT

The exchange of meteorites among the terrestrial planets of our Solar System is a well established phenomenon that has triggered discussion of lithopanspermia within the Solar System. Similarly, could solid material be transferred across planetary systems? To address this question, we explore the dynamics of the transfer of small bodies between planetary systems. In particular, we examine a dynamical process that yields very low escape velocities using nearly parabolic trajectories, and the reverse process that allows for low velocity capture. These processes are chaotic and provide a mechanism for minimal energy transfer that yield an increased transfer probability compared to that of previously studied mechanisms that have invoked hyperbolic trajectories. We estimate the transfer probability in a stellar cluster as a function of stellar mass and cluster size. We find that significant amounts of solid material could potentially have been transferred from the early Solar System to our nearest neighbor stars. While this low velocity mechanism improves the odds for interstellar lithopanspermia, the exchange of biologically active materials across stellar systems depends greatly upon the highly uncertain viability of organisms over the timescales for transfer, typically millions of years.

1. INTRODUCTION

From the collection of thousands of meteorites found on Earth, there are about 20 that have been identified as having a Martian origin, and a similar number that originated from the Moon. The study of the dynamical evolution of these meteorites agrees well with the cosmic ray exposure time and with the frequency of landing. No meteorites were ever found on the Moon by the Apollo mission. In 2005, the rover Opportunity encountered in Mars the first meteorite on another Solar System body, identified as an iron-nickel meteorite. These findings, together with dynamical simulations (Gladman 1997; Dones et al. 1999; Mileikowsky et al. 2000), indicate that meteorites are exchanged among the terrestrial planets of our Solar System at a measurable level. Because sufficiently large rocks may protect dormant microorganisms from cosmic ray exposure and from the hazards of the impact at landing, it has been suggested that the exchange of microorganisms living inside rocks could take place among the Solar System planets, a phenomenon known as *lithopanspermia*. In fact, new laboratory experiments have confirmed that several microorganisms (bacterial spores, cyanobacteria and lichen) embedded in martian-like rocks could survive under shock pressures similar to those suffered by martian meteorites upon impact ejection (Stöffler et al. 2007; Horneck et al. 2008). Under this scenario, life on Earth could potentially spread to other moons and planets within our Solar System, and/or life on Earth could have an origin elsewhere in our Solar System.

Melosh (2003) investigated the probability of lithopanspermia taking place amongst the stars in the solar local neighborhood. He found that even though numerical simulations show that up to one-third of all the meteorites originating from the terrestrial planets are ejected out of the Solar System by gravitational encounters with Jupiter and Saturn, the probability of landing on a terrestrial planet of a neighboring planetary system is extremely low because of the high relative velocities of the stars and the low stellar densities. He concluded that lithopanspermia among the current solar neighbors is "overwhelmingly unlikely".

In a subsequent paper, Adams & Spergel (2005) pointed out that the majority of stars, including the Sun[1], are born in stellar clusters with N = 100–1000 members and a typical radius of $R = 1pc(N/100)^{1/2}$ (Lada & Lada 2003 and Carpenter 2000). In such an environment, the probability of transfer would be higher due the larger stellar densities and smaller stellar relative velocities compared to those for field stars (and for the current solar

[1]In the Solar System, the existence of short-lived isotopes (^{60}Fe and ^{26}Al) in primitive meteorites has been interpreted as indication of nearby a supernova explosion shortly before the Solar System solids started to accrete. This has been considered as evidence that the Sun was born in a cluster environment.

neighborhood). The timescale for planet formation and the dispersal time of the clusters are comparable (10–100 Myr); therefore, it could be possible that solid material be transferred before the cluster disperses. Adam & Spergel (2005) estimated the probability of transfer of biologically-active remnants between planetary systems within a cluster by using Monte Carlo simulations, assuming that the stars are mostly in binary systems (which increases the cross-section). Adopting typical ejection speeds of $\sim$5 km/s, they found that the expected number of successful lithopanspermia events per cluster is $\sim 10^{-3}$; for lower ejection speeds, $\sim$ 2 km/s, this number is 1–2.

Because there is a significant increase in the number of possible lithopanspermia events with decreased ejection velocity, it is of interest to study a very low energy mechanism with velocities significantly smaller than those considered in Adams & Spergel (2005). This mechanism was described by Belbruno (2004) in the mathematical context of a class of nearly parabolic trajectories in the restricted three-body problem. The escape velocities of these parabolic-type trajectories are very low, $\sim$ 0.1 km/s, substantially smaller than the mean relative velocity of stars in the cluster, and the remnant escapes the planetary system by slowly meandering away. This process of "weak escape" is chaotic in nature and its study requires the use of methods of chaos theory, lying beyond the reach of Monte Carlo simulations employed in previous studies.

"Weak escape" is a transitional motion between capture and escape. For it to occur, the trajectory of the remnant must pass near the largest planet in the system. "Weak capture" is the reverse process, when a remnant can get captured with low velocity by another planetary system. The fact that the escape velocities of the remnants we consider here are small, enhances the probability that a remnant can be weakly captured by another planetary system due to lower approach velocities of the stars encountered.

In § 2, § 3 and § 4, we describe the mathematics of weak escape and weak capture (based on Belbruno 2004), and in § 5 we disscuss its astronomical application to the study of the slow chaotic transfer of solid material (remnants) between planetary systems within a star cluster: § 5.1 describes the location of the region supporting weak capture and weak escape for a star of a given mass; §5.2 constraints the range of stellar masses that allow minimal energy transfer (weak transfer) to take place; §5.3 estimates the probability of weak capture by a star of a given mass; and §5.4 calculates the number of weak transfer events. The focus of the paper is the study of the transfer of solid material between planetary systems, without regard to whether or not they might contain material of biological interest. Our motivation, however, is to shed light on the following questions: could the building blocks of life on Earth have been transferred to other planetary systems within the first 10–100 Myr of the Solar System evolution, when the Sun was still embedded in its maternal aggregate?; and

vice versa, could life on the Solar System have been originated beyond its boundaries? This is addressed in §5.5, where we apply the results in the previous sections to lithopanspermia, focusing in particular on solar-type stars.

2. MODEL

We first describe the mathematics of weak escape and weak capture. Readers interested in the astronomical application only could proceed to §5. We define a general planetary system, S, consisting of a central star, P_1, and a system of N planets, $P_i, i = 2, ..., N$ ($N \geq 3$) on co-planar orbits that are approximately circular. Their labeling is not reflective of their relative distances from P_1. We assume that the mass of the star, m_1, is much larger than the masses of any of the planets, m_i ($m_1 \gg m_i, i = 2, ..., N$), and that the mass of one of the planets, P_2, is much larger than the sum of the masses of all the other planets, $m_2 \gg \ m_i, i = 3, ..., N$ (this condition is fulfilled in the case of our Solar System with P_2 = Jupiter). These assumptions reduce S to a much simpler system without the loss of generality. We consider a remnant, P_0, whose mass, m_0, is negligible with respect to P_i, $i = 1, ..., N$; we assume that P_0 orbits the star in the same plane as the planets without affecting their orbits, and that it spends most of the time far from P_1. Because $m_2 \gg m_i, i = 3, ..., N$, the gravitational perturbation of P_2 on the motion of P_0 is the dominant one, and we will ignore the perturbations due to the other planets. This reduces the motion of P_0 to that of a three-body problem between P_0, P_1 and P_2, where P_1 and P_2 are moving in approximately circular orbits about their common center of mass. Because $m_1 \gg m_2$, we can view P_1 as fixed, with P_2 orbiting around it in a circular orbit at constant radial distance Δ ($1AU \leq \Delta \leq 500AU$) and orbital frequency ω. This defines the classical "planar circular restricted three-body problem" for the motion of P_0.

The differential equations for the restricted three-body problem are well known. We write them in dimensionless form; the details can be found in Belbruno (2004). Without loss of generality, we choose a reference frame with origin at the center of mass of the P_1,P_2 system; we choose units such that $\Delta = 1$, $\omega = 1$, $m_1 = 1 - \mu$ and $m_2 = \mu$, where $\mu = m_2/(m_1 + m_2) > 0$ and $\mu \ll 1$. Under these assumptions, the period of motion of P_2 around P_1 is $T = 2\pi$. We will refer to this as the reduced Solar System, S_0. In our reduced Solar System, P_1 is the Sun, P_2 is Jupiter and $\mu \approx 0.001$. In inertial coordinates (Q_1, Q_2) the differential equations for the motion of P_0 can be written as

$$\ddot{Q} = \Omega_Q, \tag{1}$$

where we have used the notation $\dot{} \equiv \frac{d}{dt}$, and $Q = (Q_1, Q_2)$, assumed to be a vector, and $\Omega_Q \equiv \frac{\partial \Omega}{\partial Q}$, with

$$\begin{aligned} \Omega &= \frac{1-\mu}{r_1} + \frac{\mu}{r_2}, & (2) \\ r_1(t) &= \sqrt{(Q_1 - \mu c)^2 + (Q_2 - \mu s)^2}, & (3) \\ r_2(t) &= \sqrt{(Q_1 + (1-\mu)c)^2 + (Q_2 + (1-\mu)s)^2}, & (4) \end{aligned}$$

where r_1, r_2 are the distances of P_0 to P_1 and P_2, respectively, $c \equiv \cos(t), s \equiv \sin(t)$, and the position of P_1 is given by $\mu(c, s)$ and that of P_2 is given by $-(1-\mu)(c, s)$.

These differential equations can also be writen in a barycentric rotating coordinate system (x_1, x_2) with orbital frequency ω. In this case, they form an autonomous system with an energy integral, the Jacobi energy, $J = J(x, \dot{x})$, where $x = (x_1, x_2)$ is a vector and J is a function on the four-dimensional phase space $(x, \dot{x})$. Along a solution, $(x(t), \dot{x}(t))$, J is a constant of the motion and defines a three-dimensional surface constraining the motion of P_0 called the Jacobi surface. In the rotating system, P_1 and P_2 are fixed and it is convenient to place them on the x_1-axis, with P_1 at $x_1 = \mu$ and P_2 at $x_1 = -1 + \mu$, in which case,

$$J = -|\dot{x}|^2 + |x|^2 + \mu(1-\mu) + 2\Omega. \quad (5)$$

where $|x|$ represents the standard Euclidian norm of x, and the additive term $\mu(1-\mu)$ is present so that the values of the Jacobi energy, $J = C$, are normalized.

3. WEAK CAPTURE AND ESCAPE

In this section, we introduce the concepts of weak capture and escape (for a detailed discussion we refer to Belbruno (2004, 2007b). A convenient way to define the capture of P_0 with respect to P_1 or P_2 is by using the concept of "ballistic capture". We define the two-body Kepler energy, E_k, of P_0 with respect to one of the bodies $P_k, k = 1, 2$:

$$E_k = \frac{1}{2}v^2 - \frac{m_k}{r_k} \quad (6)$$

where v is the velocity of P_0 relative to P_k. Ballistic capture takes place when $E_k \leq 0$. More precisely, let $\phi(t) = (Q(t), \dot{Q}(t))$ be a solution of Eq.(1) for P_0, and assume no collisions take place, i.e. $r_k > 0$. P_0 is ballistically captured by P_k at time $t = t^*$ if $E_k(\phi(t^*)) \leq 0$; similarly, P_0 escapes P_k at time $t = t_2$, if there exists a finite time interval $[t_1, t_2]$, with $t_2 > t_1$ where $E_k(\phi(t_1)) \leq 0$ and $E_k(\phi(t_2)) > 0$. For notation, we set $E_k(\phi(t)) = E_k(t)$.

Now we consider the motion of P_0 around P_2 (this is known as Hill's problem). If the motion of P_0 is initially circular and occurs sufficiently close to P_2, it is found that the motion is generally stable and E_2 remains negative for all times (this was proven by Kummer(1983) applying the Kolmogorov-Arnold-Moser theorem). However, if P_0 is not sufficiently near to P_2, then the stability will break down and the motion will substantially deviate from a circular orbit, leading to escape from P_2 due to the gravitational perturbation of P_1.

Of particular interest is temporary ballistic capture. This occurs when P_0 is ballistically captured by P_2 over the finite interval $[t_1, t_2]$, i.e., when $E_2(t) \leq 0$, for $t_1 \leq t \leq t_2$, $E_2(t_1) = 0, E_2(t_2) = 0$, and $E_2(t) > 0$ for $t < t_1$ and $t > t_2$. We say that P_0 is "pseudo-ballistically captured" at a time $t = t^*$ when $E_2(t^*) \gtrsim 0$, i.e. where the Kepler energy is slightly hyperbolic.

Because temporary ballistic capture with respect to P_2 is generally unstable and chaotic in nature (Belbruno 2004; Garcia & Gomez 2007) and lies at the transition between capture and escape, it is referred to as "weak capture". For weak capture to occur, the Jacobi energy C must be small enough so that the velocity of P_0 is sufficiently large at a given distance from P_2 to be in this transition state.

As is evident by numerical integration of P_0 about P_2, weak capture generally occurs for relatively short time spans, $\Delta t = t_2 - t_1$. For example, in the case of the Earth-Moon system ($\mu = 0.012$), weak capture about the Moon occurs for time spans of days or weeks; in the case of the Sun-Jupiter system, the timescale is months or a few years (Belbruno & Marsden 1997; Belbruno 2007a)

A numerical approach to estimate the region around the Moon supporting weak capture was developed by Belbruno (2004). This region was termed the weak stability boundary, $\mathcal{W}$, and it is the location in the phase space where the motion of P_0 with respect to P_2 lies between capture and escape. Recent results by Garcia & Gomez (2007) have precisely determined $\mathcal{W}$ using the numerical approach and have shown that it is closely related to a complicated fractal region in phase space supporting unstable chaotic motion. However, the location of $\mathcal{W}$ can be can be approximately estimated analytically in a straight forward manner by a set W described as follows:

Consider the barycentric rotating coordinates $x = (x_1, x_2)$. To be in weak capture, P_0 must have a suitably large velocity magnitude, $|\dot{x}|$, that depends on the velocity direction at a given distance r_2 from P_2. This is equivalent to the requirement that the Jacobi constant C needs to be in a suitably small range: we require that $C \lesssim C_1$, where C_j is the value of J at the classical Lagrange points L_j (which are the locations at which $|\dot{x}| = 0$). We label the three collinear Lagrange points from left to right (in the rotating barycentric reference

frame defined in § 2) with index 1,2, and 3; then the values of the Jacobi energy, C_j, at each of these points has the ordering: $C_2 > C_1 = 3$. As C decreases, the allowed range of motion, x, of P_0 expands. When C goes just below C_1, the Hill's region[2] around P_2 opens near the position of L_1 so that P_0 can move out of the Hill's region around P_2, and infinitely far away from both P_1 and P_2 (see Figure 1 – i.e. C_1 is the minimal Jacobi energy for escape). If we decrease C further, $C < 3 < C_1$, then the zero velocity curves disappear and the Hill's region becomes the entire x_1x_2-plane.

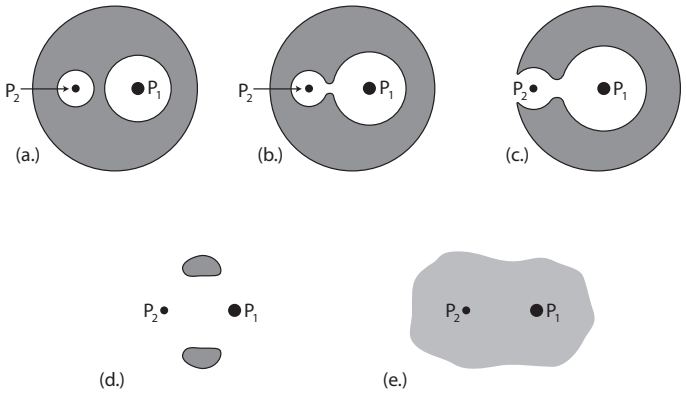

Fig. 1.— Basic Hill's regions (in *white*): Starting from left to right and top to bottom, C has the values: $C > C_2; C_1 < C \lesssim C_2; C \lesssim C_1$; $C_3 < C < C_1$ and $C < 3$.

As is described in Belbruno (2004), the set W has two components, W_E and W_H, as follows.

$$W = W_E \cup W_H, \tag{7}$$

$$W_E = \{(x, \dot{x}) \in \mathbb{R}^4 | E_2 \leq 0, J = C, C^* \leq C < C_1, \dot{r}_2 = 0\}, \tag{8}$$

$$W_H = \{(x, \dot{x}) \in \mathbb{R}^4 | E_2 \gtrsim 0, J = C, C^* \leq C < C_1\}, \tag{9}$$

where the constant C^* is determined so that W exists and depends on the value of μ. Weak capture occurs on W_E (associated with osculating elliptic orbits about P_2), and pseudo-ballistic capture (equivalently pseudo-ballistic escape) occurs on W_H (associated with slightly hyperbolic orbits),

For weak capture we need to consider the set W_E,

$$W_E = \mathcal{J}(C) \cap \Sigma \cap \sigma, \tag{10}$$

[2]The Hill's region for a given value of C is the projection of the Jacobi surface onto the x_1, x_2 space, which yields locations where P_0 is allowed to move.

where $\mathcal{J} = \{(x, \dot{x}) \in \mathbb{R}^4 | J = C\}$, $\Sigma = \{(x, \dot{x}) \in \mathbb{R}^4 | E_2 \leq 0\}$, $\sigma = \{(x, \dot{x}) \in \mathbb{R}^4 | \dot{r}_2 = 0\}$. W_E is equivalent to a set of osculating elliptic orbits about P_2 with osculating pericenter q_2, in a two-dimensional annular region described by

$$q_2 = f(\theta_2, e_2), \tag{11}$$

where θ_2 ($0 \leq \theta_2 \leq 2\pi$) is the polar angle measured with respect to the P_1,P_2 axis) in a P_2-centered rotating coordinate system, the function f is periodic in θ_2 of period 2π, and e_2 is the osculating eccentricity of the orbit of P_0 with respect to P_2 ($0 \leq e_2 \leq 1$). For example, in the case where $C \lesssim C_1$ and $q_2 \gtrsim 0$,$\mu \gtrsim 0$, this relationship takes the form,

$$q_2 \approx \frac{(1 - e_2)\mu^{\frac{1}{3}}}{3^{\frac{5}{3}} - \frac{2}{3}\mu^{\frac{1}{3}}}. \tag{12}$$

The set W_H plays a key role on the existence of chaos, as it is proven that a hyperbolic invariant set associated to parabolic motion with respect to P_1 exists on the set W_H, giving rise to chaotic dynamics (Belbruno 2004, pages 186-191).

A more accurate estimation of $\mathcal{W}$ has recently been obtained for a large range of the Jacobi energies by Belbruno et al. (2007b) through the visualization of special two-dimensional Poincaré sections, generally showing resonant tori lying within a chaotic sea. These sections yield a more accurate representation of $\mathcal{W}$, suggesting that it may consist of transverse homoclinic points, related to the intersections of the invariant manifolds of the Lyapunov periodic orbits associated to the unstable Lagrange points. It is demonstrated that during weak capture, P_0 moves around P_1 while transitioning between various resonant states with respect to P_2. However, these results apply to elliptic-like resonant motions that are not sufficiently energetic for the purposes of this paper. In the following, we will be considering the parabolic motions associated with W_H.

In our Solar System, the existence of the weak stability boundary and the viability of weak capture was demonstrated in practice by the Japanese spacecraft *Hiten*: using a trajectory designed by Belbruno (1990, 1993, 2007a), *Hiten* was captured into an orbit around the Moon in 1991 without the use of rockets to slow down. Weak capture at the Moon was also achieved in 2004 by the ESA spacecraft *SMART1* (Racca 2003, Belbruno 2007a). In both cases, the capture was chaotic and unstable because the orbit lay in the transition between capture and escape. In another application, weak escape from the Earth's L_4 (or L_5) was invoked to suggest a low energy transfer to the Earth for the hypothetical Mars-sized impactor that is thought to have triggered the "giant impact" origin of the Moon (Belbruno & Gott 2005).

4. PARABOLIC MOTION AND CHAOS

In this section, we describe the mechanism for low velocity escape from S that is chaotic and applies to the set of parabolic trajectories around P_1. The reverse process yields low velocity chaotic capture into S. Consider a solution $Q(t)$ of (1) for P_0 in the case of the reduced Solar System S_0 for the restricted three-body problem: P_0 is on a parabolic trajectory with respect to P_1 when $\lim_{t\to\pm\infty}|Q| = \infty$ and $\lim_{t\to\pm\infty}|\dot{Q}| = 0$. In the absence of any of the planets, the motion of P_0 is that of a standard parabola around P_1, and the Jacobi energy has the value $C = \pm 2\sqrt{2}$, where + is for retrograde parabolic trajectories, and – is for direct trajectories.

In the case of the Solar System, S, because the masses of the planets are very small with respect to that of P_1, the motion of P_0 will be slightly perturbed and the trajectories that lie very close to parabolic trajectories will be able to escape P_1 with very small velocities; we refer to these as "pseudo-parabolic trajectories". These trajectories satisfy $|Q| \to R$, $|\dot{Q}| \to \sigma$, as $t \to T_R$, and, without loss of generality, we assume that P_0 started at periapsis with respect to P_1 at time $t = 0$ and traveled a distance R in a sufficiently long time $T_R > 0$. The value of σ is small and coincides with the escape velocity with respect to P_1 at the distance R, $\sigma = \sqrt{2Gm_1/R}$; R is chosen sufficiently large so that P_0 can escape S when it has a velocity close to σ.

For notational purposes, the term "parabolic trajectory" refers to the solution of (1) for S_0 in scaled dimensionless coordinates and the precise definition of parabolic motion; whereas, when using the term "pseudo-parabolic trajectory", we are considering system S in unscaled dimensional coordinates. We now describe the main results for S_0, followed by the results for S.

Main Results for S_0:

Let $\phi(t) = (Q(t), \dot{Q}(t))$ be a parabolic solution of (1) for P_0 in a system where $\mu = 0$ and where P_0 does not collide with P_1 (i.e. $r_1 > 0$). Consider the set of parabolic trajectories with $|C| \lesssim 2\sqrt{2} \approx 2.83$, that pass through the location of P_2 (now with zero mass because $\mu = 0$). Belbruno (2004) found that for $0 \leq \mu \ll 1$, if P_0 passes sufficiently close to P_2 without collision ($r_2 > 0$) and slightly beyond the distance Δ, then: (a) when P_0 passes close to P_2, it is slightly hyperbolic and in the set W_H (i.e. pseudo-weakly captured) around P_2; (b) P_0 never collides with P_1 or P_2; (c) the periapsis location of P_0 with respect to P_2 is approximately the periapsis location with respect to P_1; (d) there exists a set of positive measure of parabolic trajectories (i.e. parabolic trajectories exist); and (e) the motion of P_0 is chaotic.

There are two possible outcomes:

1. P_0 parabolically escapes P_1, i.e. $|Q| \to \infty$ and $|\dot{Q}| \to 0$ as $t \to \infty$.
2. P_0 does not escape but instead, after traveling a large finite distance, falls back towards P_1, passing again by P_2 in a slightly hyperbolic orbit w.r.t P_2 in which P_0 is pseudo-weakly captured by P_2, after which it flies around P_1 and out again toward $|Q| = \infty$.

In the second case, every time P_0 falls back to fly by P_2, the argument of periapsis of the pseudo-parabola with respect to P_1 is chaotic in nature and can take on a random value. If P_0 were to keep falling back to P_2 again and again, it would be permanently captured by P_1. However, it can be proven that this does not happen (in mathematical terms this is because the set of orbits leading to permanent capture are of zero measure); on the contrary, escape eventually takes place (i.e. there is a set of positive measure of parabolic trajectories that will escape to infinity after flying by P_2). In addition, in this case, there is a constraint on the fly-by distance q_2 as a function of μ. If we consider the case of a direct fly by, the velocity of P_0 with respect to P_1 when it flies by P_2 is $V \approx 1.414$ (in dimensionless units) – this is because the fly-by is close to P_2 and therefore has a distance $\Delta \approx 1$ to P_1, and hence, $V \approx \sqrt{2/\Delta} \approx 1.414$); therefore, the velocity of P_0 with respect to P_2 is approximately 0.414, and the Kepler energy of P_0 with respect to P_2 is $E_2 \approx 0.08 - (\mu/r_2)$. A slight hyperbolic fly-by implies that $E_2 \gtrsim 0$, or equivalently, $r_2 \gtrsim \frac{\mu}{0.08}$. In the case of the Solar System, if P_2 is Jupiter ($\mu = 0.001$) then $r_2 \gtrsim 0.013$ = 10,172,800 km, while for Neptune ($\mu = 0.00005$), $r_2 \gtrsim 0.0006$ = 2,692,800 km.

Main Result for S:

The parabolic motion previously described for P_0 in the system S_0 can be translated to the pseudo-parabolic motion of P_0 in the system S in the following manner. There is a set of positive measure of pseudo-parabolic trajectories with respect to P_1 that pass by P_2 without colliding with it, and where P_0 is slightly hyperbolic with respect to P_2. The motion of such trajectories is sensitive due to the fly-by. As P_0 approaches P_2, it achieves a periapsis with respect to P_2 slightly beyond P_2's orbit, with energy at periapsis slightly hyperbolic with respect to P_2. At that location, it is also approximately at the periapsis with respect to P_1. P_0 then flies outward away from P_1 for a long period of time T_R, reaching a distance R with a velocity $\sim \sigma$. P_0 pseudo-parabolically escapes P_1 with approximate parabolic escape velocity magnitude σ, when r_1 increases beyond R as t increases beyond T_R.

Weak Stability Boundary Around P_1

The pseudo-parabolic escape of P_0 occurs for R sufficiently large so that the gravitational perturbation in P_2 is negligible. We have a two-body problem between P_0 and P_1, where P_0 is moving with a small velocity σ. We can define a weak stability boundary about P_1. This can be accomplished by considering a situation where the star P_1 is not isolated but included within a star cluster. We can think of a new "three-body problem" consisting of P_1, P_0, and a third object, B, that mimics the combined gravitational forces from the neighboring stars in the cluster. The gravitational perturbation of B together with the gravity of P_1 forms a weak stability boundary region far from P_1 that is located at a finite distance that depends on the characteristics of the cluster and the separation of the stars. P_0 lies in the transition between capture and escape from P_1, when R is sufficiently large and σ is sufficiently small.

5. REMNANT TRANSFER BETWEEN STELLAR SYSTEMS IN OPEN STAR CLUSTERS

Using the framework discussed in the previous sections we now consider the problem of remnant transfer between planetary systems in star clusters with low velocity dispersion, since low relative velocities are required for the weak capture mechanism. Specifically, we consider open clusters which typically have low relative stellar velocities, $U \approx 1$ km/s. For comparison, we note that in older globular clusters, stellar velocity dispersion can reach many 10's of km/s. Also for comparison, we mention that when a cluster starts to disperse, the relative distances and relatives velocities between the Sun and neighboring stars increase. For example, in the solar neighborhood, the Sun's closest neighbor α-Centauri is 2.6×10^5 AU away (1.28 pc) with a relative velocity of 6 km/s. The latter is significantly higher than the ~ 1 km/s required for weak capture, making the transfer of material between the two stars very unlikely via weak transfer. Therefore, we will consider relatively young open clusters.

We assume that the stars in the open cluster are approximately uniformly spaced in a three-dimensional grid by a distance D and that their distribution is isotropic. Imagine a remnant (P_0) in a planetary system (S) passing near the primary planet (P_2) having a weakly hyperbolic flyby, moving away from the star (P_1) on a pseudo-parabolic trajectory, and reaching a distance $R = R_{esc}(m_1)$ from the star. At this distance, the small gravitational force acting on the remnant due to the central star is roughly comparable with the resultant gravitational force from the other stars in the cluster, as described above; as a consequence, the motion of the remnant becomes unstable, with small changes to its velocity leading to large changes in its trajectory that can either lead to capture or escape from the central

star[3]. In other words, the sphere of radius R around the central star lies within a weak stability region and can be thought of as a uniform slice through the more complicated weak stability region.

As shown in Figure 2, due to the structure of the space of parabolic trajectories, for any point p on the circle of radius $R_{esc}(m_1)$ around the star P_1, there is a weakly-escaping trajectory that will pass by p with velocity σ moving away from the star (see also Figure 1 in Moro-Martín & Malhotra 2005). Assume that the point p lies on the line between the two stars. As the remnant (P_0) passes through this point and moves beyond the distance $R_{esc}(m_1)$ from the star, it goes beyond its weak stability boundary, moving to a region where the gravitational force of the star is negligible. The trajectory then continues undisturbed until the remnant moves within the weak stability boundary of another star, P_1^* in planetary system S^*, located at a distance $R_{cap}(m_1^*)$ from P_1^*. The remnant can then get captured by P_1^*, with a periapsis distance that is minimally a collision or maximally a distance $R_{cap}(m_1^*)$ from P_1^*.

Analogous to planetary system S, we are assuming that S^* has a dominant planet P_2^* at a radial distance Δ^* from the star P_1^* (see Figure 2). For weak escape to occur, it is necessary that the remnant P_0 weakly escapes the star P_1 in the same plane of motion as that of the dominant planet P_2, and that the periapsis distance, r_p, of P_0 with respect to P_1 is approximately the semi-major axis of the dominant planet, $\Delta \approx r_p$. However, when P_0 is weakly captured by P_1^* and moves to periapsis distance r_p^* with respect to P_1^* ($0 \leq r_p^* \leq R_{cap}(m_1^*)$), it need not approach this periapsis within the same plane of motion as the dominant planet P_2^*. This capture into S^* is three-dimensional in nature and the remnant P_0 can approach the star P_1^* from any direction.

The construction of the transfer from the periapsis with respect to P_1 (and also P_2) to the periapsis with respect to P_1^* can be approximated by determining a solution for P_0 in a five-body problem between P_0, P_1, P_2, P_1^* and P_2^*. We can approximate it by piecing together the solutions between two three-body problems, P_0, P_1, P_2 (hereafter TB1), and P_0, P_1^*, P_2^*

[3]The sensitivity of the motion of P_0 at the distance R can be deduced from an analogous four-body problem described in Belbruno (2004) and Marsden & Ross (2006) for a transfer to the Moon used by the spacecraft *Hiten*. In this case, the four bodies are the Earth (P_1), the Moon (P_2), the Sun (P_3) and the spacecraft (P_0). The spacecraft leaves the Earth and travels out to roughly 1.5×10^6 km where the gravitational force of the Sun acting on the spacecraft approximately balances that of the Earth. At this location, the motion of the spacecraft is highly sensitive to small differences in velocity, and lies between capture and escape from the Earth, i.e. lies at the weak stability boundary between the Earth and Sun. The spacecraft then falls back towards the Earth and the Moon entering the weak stability boundary between the Moon and the Earth, which finally leads to capture by the Moon.

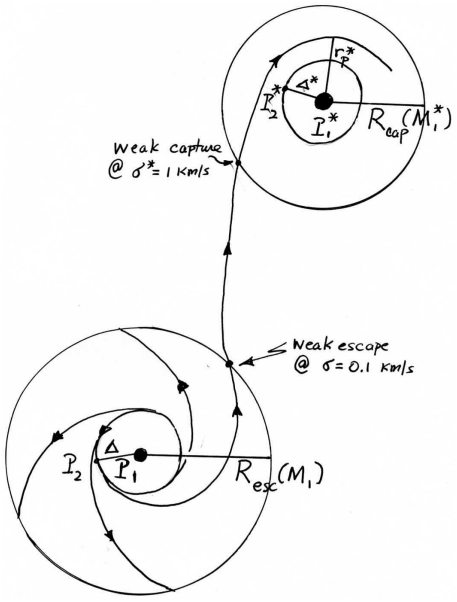

Fig. 2.— Trajectory weakly escaping P_1 at a distance $R = R_{esc}(m_1)$, being weakly captured by P_1^* at a distance $R = R_{cap}(m_1^*)$, and moving to periapsis with respect to P_1^* (motion projected onto a plane).

(hereafter TB2). This is done as follows. We know that pseudo-parabolic trajectories in the first three-body problem, $TB1$, exist as described above. In fact, the theory of their existence proves there is an infinite number of them, forming the structure of a Cantor set, that will travel out to a distance $R_{ecs}(m_1)$ where the gravitational perturbation due to $TB2$ begins to be felt and where the dynamics of P_0 becomes sensitive. The velocity of P_0 at this distance is approximated by the escape velocity from P_1. That is, P_0 weakly escapes the first system. Let's assume that P_0 is then weakly captured by $TB2$. Its velocity magnitude would then approximately be the escape velocity from P_1^* at the given distance, $R_{cap}(m_1^*)$. If P_0 were moving in the same plane as P_2^* about P_1^*, then by the same theory on pseudo-parabolic trajectories, there would exist, by symmetry, an infinite number of trajectories that are weakly captured into the system $TB2$ and fly by P_2^* in slight hyperbolic state. Then, a capture trajectory can be generated in forwards time as an extension of the the weak escape trajectory starting at a distance $R_{cap}(m_1^*)$ from P_1^*. If, on the other hand, the trajectory of P_0 does not lie in the same plane of motion of P_2^* when it is weakly captured by P_1^*, then the theoretical results on pseudo-parabolic trajectories cannot be applied. However,

the trajectory of P_0 can still be extended in forwards time and will move towards P_1^* and fly by P_2^*. In this case, it cannot be guaranteed that P_0 will fly by P_2^* in a weakly hyperbolic manner, although it would be reasonable that this would occur if the time of capture into $TP2$ were sufficiently long. More precisely, one of the following would occur:

(i) P_0 remains in a bounded region about P_1^* without collision with P_1^*. Then by the Poincaré recurrance theorem, P_0 would eventually fly by P_2^* in a slight hyperbolic fashion or collide with P_2^*

(ii) P_0 collides with P_1^*

(iii) P_0 is ejected from the $P_1^* - P_2^*$- system.

The piecing together of solutions at the weak stability boundary regions, for different types of trajectories, is discussed in Belbruno 2004 and Marsden & Ross 2006). The piecing together occurs at the weak stability boundaries of $TB1$ and $TB2$.

5.1 Location of the Weak Stability Boundary

We now calculate $R_{esc}(m_1)$ and $R_{cap}(m_1^*)$ as a function of the stellar mass. For weak escape to take place, the velocity, σ, of the remnant at the distance $R_{esc}(m_1)$ from the star P_1 must be sufficiently smaller than the escape velocity at that distance from P_1 as well as the other stars in the cluster; i.e. it is on the weak stability boundary. At this distance the gravitational forces from P_1 and from the other stars in the cluster are comparable, and the motion of the remnant is unstable and chaotic in nature. Because we are considering slow transfer within an open cluster with a characteristic dispersion velocity $U \approx 1$ km/s, we require that σ is significantly smaller than U, i.e. of the order of 0.1 km/s. This is much smaller than the nominal values of several km/s used by the Monte Carlo methods in previous studies (e.g. Melosh 2003, Adams & Spergel 2005).

To place the above choice for σ in context, we study the velocity distribution of weakly escaping test particles from the Solar System, using a three-body problem between the Sun (P_1), Jupiter (P_2) and a massless particle (P_0). To be consistent with our framework, we model this as a planar circular restricted three-body problem, where the test particle moves in the same plane of motion as Jupiter, assumed to be in a circular orbit at 5 AU. The trajectory of the test particle is numerically integrated by a standard Runge-Kutta scheme of order six and numerical accuracy of 10^{-8} in the scaled coordinates. The initial conditions of the test particle is an elliptic trajectory very close to parabolic with periapsis distance

r_p=5 AU and apoapsis distance r_a=40,000 AU. (Note that such orbits are not dissimilar to those of known long period comets in the Solar System.) For each numerical integration, we assume that Jupiter is at a random point in its orbit when the test particle starts from apoapsis at 40,000 AU and falls towards P_1. We record the time at which the test particle achieves escape with respect to the Sun (i.e. when the Kepler energy with respect to the Sun is positive) after performing a sufficient number of Jupiter fly-bys, and we record the resulting hyperbolic excess velocity v_∞. Figure 3 shows the distribution of the v_∞: out of 670 cases, 58% have $v_\infty \leq 0.1$ km/s and 79% have $v_\infty \leq 0.3$ km/s. Based on these results we will assume the velocity σ of the remnant at the distance $R_{esc}(m_1)$ from the star to be in the range 0.1–0.3 km/s.

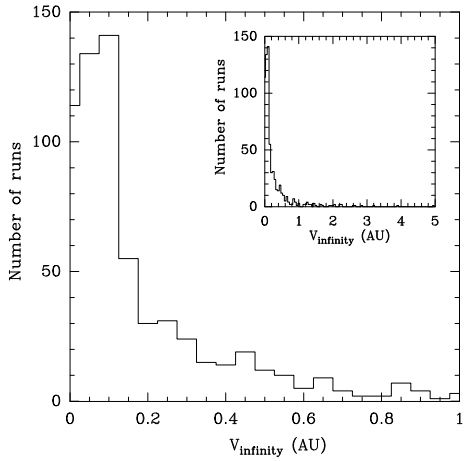

Fig. 3.— Velocity distribution of weakly escaping test particles from the Solar System. The model is a planar circular restricted three-body problem between the Sun, Jupiter and a massless particle.

For a given σ, the location of the weak stability boundary is approximately given by $R_{esc}(m_1) = 2Gm_1/\sigma^2$, where m_1 is the mass of the star and σ is in the range 0.1–0.3 km/s (see Figure 4). Beyond this boundary, we assume that the remnant will move at a constant velocity σ with respect to the star.

To allow slow chaotic transfer to a neighboring planetary system, the remnant needs to arrive at the distance $R_{cap}(m_1^*)$ with a relative velocity with respect to the target star (P_1^*) that is similar or smaller than its parabolic escape velocity at that distance, $\sigma^* = \sqrt{2Gm_1^*/R_{cap}(m_1^*)}$, where m_1^* is the mass of the target star; if its velocity is higher than σ^* it will not be captured and and will fly by. Since the relative velocity between stars in the cluster is $U \approx 1$ km/s, the remnant that weakly escaped from star P_1 moves toward

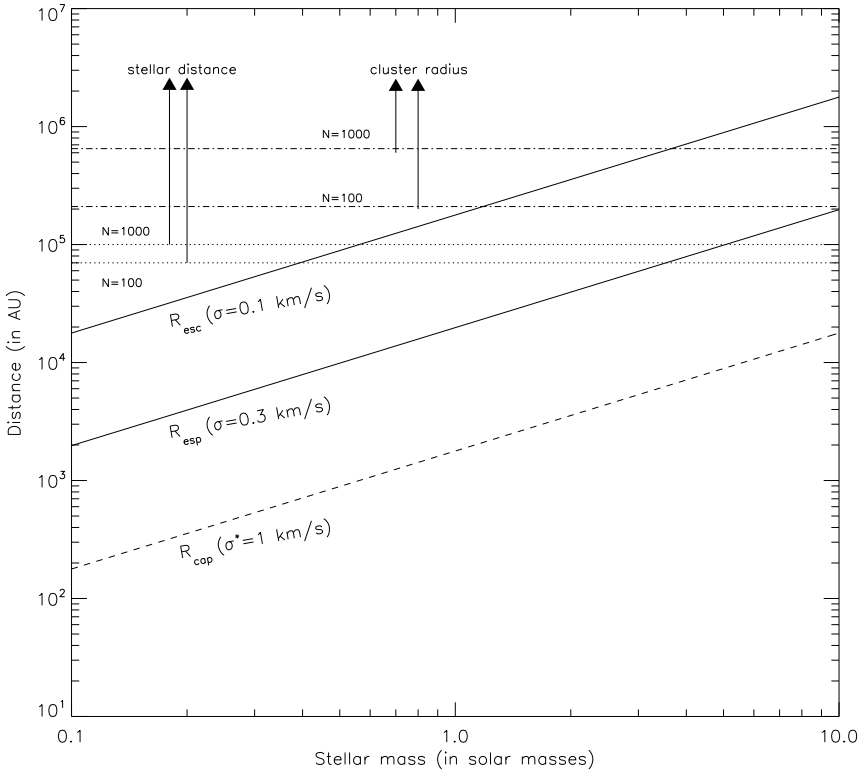

Fig. 4.— Radius of the weak stability boundary as a function of stellar mass. The weak escape boundary is defined as $R_{esc}(m_1) = 2Gm_1/\sigma^2$ with $\sigma = 0.1$–0.3 km/s, and the weak capture boundary is at $R_{cap}(m_1^*) = 2Gm_1^*/U^2$ with $U = 1$ km/s. The horizontal dashed-dotted line indicates the range of cluster sizes, while the dotted line indicates the the mean interstellar distance in clusters consisting of N=100 and N=1000 members.

the target star P_1^* with velocity $U \pm \sigma$ (see Figure 2). Because σ is small relative to U and can be neglected, the relative velocity of the remnant with respect to the target star is $\approx U$. Therefore, weak capture can occur at the distance at which $\sigma^* \approx U \approx 1$ km/s, i.e. $R_{cap}(m_1^*) = 2Gm_1^*/U^2$.

Figure 4 shows $R_{esc}(m_1)$ and $R_{cap}(m_1^*)$ as a function of the stellar mass. The horizontal dotted lines indicate the range of cluster sizes and mean interstellar distances for clusters consisting of 100 and 1000 members, respectively; such clusters are the birthplaces of a large fraction of stars in the Galaxy. The radius of the cluster depends on the number of stars, N, and is given by

$$R_{\rm cluster} = 1pc(N/100)^{1/2}. \tag{13}$$

$R_{\rm cluster}$ is about 2.1×10^5 and 6.5×10^5 AU for N=100 and N=1000 members, respectively (based on data in Lada & Lada 2003 and Carpenter 2000, and following Adams & Spergel 2005). We can estimate the average interstellar distance within a cluster,

$$D = n^{-1/3}, \tag{14}$$

where $n = 3N/(4\pi R^3_{\rm cluster})$ is the average number density of stars in the cluster. D is about $7{\times}10^4$ AU and 10^5 AU for a cluster with N=100 and N=1000 members, respectively.

5.2 Constraints on Stellar Masses for Weak Transfer

From Figure 4 we can set constraints on the stellar mass m_1 that could allow weak escape from P_1 to take place. The idea is simple: if for a given σ (which as we saw in § 5.1 is in the range 0.1–0.3 km/s), $R_{esc}(m_1) < D$, i.e. the weak stability boundary is located within the distance of the next neighboring star P_1^*, then weak transfer is possible because at the time the remnant passes near the star P_1^*, its velocity is similar to the mean stellar velocity dispersion, U (which is a low ~ 1 km/s in open clusters), and there is a significant probability of capture (which we quantify in the next section). Conversely, neighbor transfer by the process schematically represented in Figure 2 is much less likely to take place if $R_{esc}(m_1) > D$ because at the time the remnant passes near a neighboring star, its velocity is too high and as a consequence it will simply fly by.

Consider $\sigma = 0.1$ km/s. Figure 4 shows that for clusters with 100 members, the condition $R_{esc}(m_1) < D$ for weak escape is satisfied for $m_1 < 0.4 M\odot$, and for clusters with 1000 members, the condition is satisfied $m_1 < 0.55 M\odot$. If we consider the higher but still acceptable value $\sigma = 0.3$ km/s, Figure 4 shows that the stellar mass limits for weak escape are $m_1 < 3.5 M_\odot$ and $m_1 < 5 M_\odot$ for clusters of 100 members and of 1000 members, respectively. A remnant escaping parabolically from any star with larger mass than these limits will achieve a velocity of $\sigma < 0.1$–0.3 km/s only at a distance larger than the mean interstellar distance in the cluster and weak transfer is not likely under such conditions.

Of particular interest is the case of the Sun as the source of the remnants. It has been estimated that the Sun's birth cluster consisted of $N = 2000 \pm 1100$ members (Adams & Laughlin 2001). For a $1 M_\odot$ star in such a cluster, we find that the parabolic escape velocity at the mean interstellar distance is $\sigma \simeq 0.12$–0.14 km/s. These values of σ certainly lie within the range of values of interest for weak escape. We conclude that *remnants originating in the early Solar System could in principle have met the conditions for weak escape in the Sun's birth cluster.*

5.3 Probability of Weak Capture

We have established in §5.2 the range of stellar masses that could in principle allow weak escape to take place, we now estimate *roughly* the probability of capture by a neighboring planetary system.

As mentioned previously, because the trajectory of the remnant approaching the target system S^* is not necessarily in the same plane as that of the orbit of its primary planet P_2^*, and because the capture can be complicated (where P_0 could be captured for millions of years, moving in a complicated trajectory without planetary collisions), capture is not guaranteed even if the renmant P_0 falls within the weak stability boundary of the target star P_1^*. However, because a necessary condition for capture is that the renmant lies within this weak stability boundary, we can use the following geometrical considerations to set an *upper limit* for the capture probability. Whether or not the transfer of remnants from one star to any star of mass m_1^* takes place will depend on:

1. *The relative capture cross-section of the target star.*

   This is given by $C_S = G_f(R_{cap}(m_1^*)/D)^2$, where D is the distance between the two stars and R_{cap} is described in §5.1 and Figure 4 (dashed line). The factor G_f represents the gravitational focusing, given by

   $$G_f = 1 + (\frac{v_{esc}}{v_\infty})^2, \tag{15}$$

   where v_∞ is the velocity at infinity and v_{esc} is the escape velocity at the distance $R_{cap}(m_1^*)$ from P_1^*.

   In the case of weak capture, the term G_f increases the cross-section due to enhanced gravity focusing. For example, as we saw previously in the case of the Sun and Jupiter, $v_\infty \approx 0.1 - 0.3$ km/s, while at the distance $R_{cap} = 40,000$ AU, $v_{esc} \approx 0.2$ km/s. Therefore, in this example, $G_f \approx 2$, which doubles the capture cross-section. This situation occurs in our capture methodology. In the formulation for determining $R_{cap}(m_1^*)$, the remnant has an approximate relative approach velocity to the target star P_1^* of roughly $U = 1$ km/s, which represents the v_∞. However, R_{cap} is determined so that this same value of velocity is taken for v_{esc} from the target star. That is, we are assuming, $v_\infty \approx v_{esc} \approx 1$ km/s. This implies also that $G_f = 2$. This is a conservative estimate and does not make use of the nature of weak capture dynamics. In this situation, we have a trajectory with a $v_{inf} = 1$ with respect to P_1^*, which goes to a parabolic state with respect to P_1^*.

As noted, the value $G_f = 2$ is conservative. In principle, the value of G_f could be substantially increased if at a given value of $R_{cap}(m_1^*)$, v_∞ is smaller than the approximate value of $U = 1$ km/s, while the value of v_{esc} remains the same as U. Dynamically, the way to decrease the v_∞ with respect to P_1^*, as the remnant P_0 approaches P_1^*, is for P_0 to decrease its relative velocity. This process has been shown to exist in other problems; for example, in the case where we have a spacecraft, P_0, transferring from the Earth to the Moon on a trajectory that goes to ballistic capture at a given distance from the Moon (demonstrated by spacecraft as was discussed previously). Figure 5, shows a trajectory to the Moon, going to a periapsis distance of 500 km after 111 days. When it arrives its velocity is approximately v_{esc}. However, its v_∞ goes from a value of 1 km/s to 0. This is reflected in Figure 6 of the Kepler energy K_M of P_0 with respect to the Moon along this transfer. At a sufficiently far distance from the Moon, where $v_\infty \approx \sqrt{2K_E}$, v_∞ approaches zero. In the future, we would like to examine the distribution of the v_∞ in the WSB about P_1^* and thereby get a better understanding of the G_f and the enhanced capture probabilities.

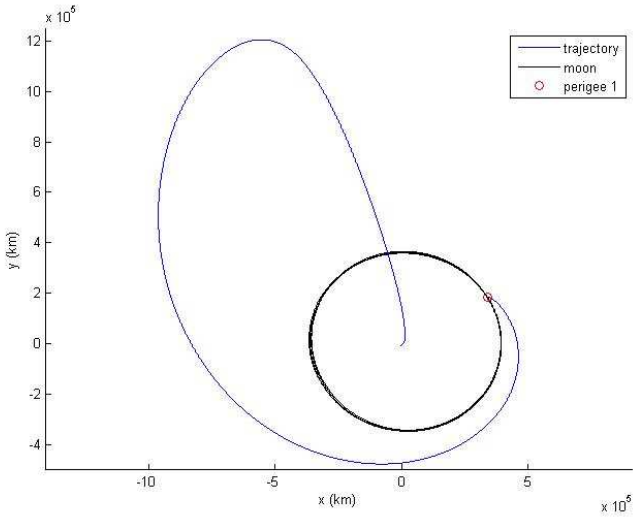

Fig. 5.— Trajectory from the Earth to the Moon going to the lunar WSB.

2. *The number of potential targets.* This depends on the probability of finding a star of a given mass m_1^* in the cluster; we call this $P_{IMF}(m_1^*)$ which describes the initial mass function (IMF) of the cluster. Observations of many different star clusters (large clusters like the Trapezium, smaller cluster like Taurus and even older field stars) find very similar IMFs (down to the Hydrogen burning limit at $\sim 0.1\ M_\odot$; Lada & Lada 2003 and refereces therein). To calculate $P_{IMF}(m_1^*)$ we adopt the IMF of the Trapezium

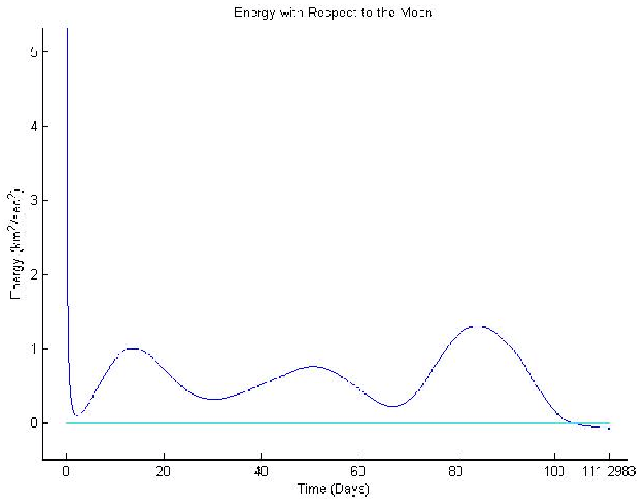

Fig. 6.— Caption: Variation of the Kepler energy, K_M.

cluster from Lada & Lada (2003), which is characterized by a broken power-law, given by $\xi(\mathrm{M}) = \xi_1 \mathrm{M}^{-2.2}$, from 0.6–20 $M_\odot$ and $\xi(\mathrm{M}) = \xi_2 \mathrm{M}^{-1.1}$, from 0.1–0.6 $M_\odot$, where $\xi(\mathrm{M})\mathrm{dM}$ is the number of stars with mass (M, M+dM). [There is a steep decline into the substellar brown dwarf regime and a possible second peak but we will ignore objects below the hydrogen burning limit]. To calculate $P_{IMF}(m_1^*)$ (square symbols in Figure 7), we use a logarithmic binning of masses (with d(logM)=0.1), and normalize the distribution to unity, which gives ξ_1=0.19 and ξ_2=0.34.

An upper limit to the probability that a remnant escaping from a star of mass m_1 (within the range described in §5.1) will get captured by a neighboring star of mass m_1^* is approximately given by $2(R_{cap}(m_1^*)/D_{m_1^*-m_1})^2$, where $D_{m_1^*-m_1}$ is the average distance between two stars of masses m_1^* and m_1, respectively. The simplest case is when both stars have equal masses $m_1^* = m_1$. In this case, the average interestellar distance would be $D_{m_1} \sim (1/n_{m_1})^{1/3}$, where n_{m_1} the average number density of stars with mass m_1, $n_{m_1} = N_{m_1}/(4/3)\pi R^3_{cluster}$, and N_{m_1} is the total number of stars in the cluster with mass m_1, $N_{m_1} = N \times P_{IMF}(m_1)$. Because $n_{m_1} = n \times P_{IMF}(m_1)$, we get that $D_{m_1} \sim D \times (P_{IMF}(m_1^*))^{-1/3}$. This means that the transfer probability between two stars of equal mass is given by $2(R_{cap}(m_1^*)/D)^2 \times (P_{IMF}(m_1^*))^{2/3}$, where D is the average distance between any two stars in the cluster (regardless of their mass). The resulting capture probability is shown in Figure 7 as a solid line, with values ranging from 10^{-6} to 10^{-3}. The capture probability between two planetary systems with solar-type central stars ($\mathrm{M}_1^* = \mathrm{M}_1 = 1\ M_\odot$) is $8.1{\times}10^{-5}$ and $1.7{\times}10^{-4}$, for a cluster of 1000 and 100 members, respectively.

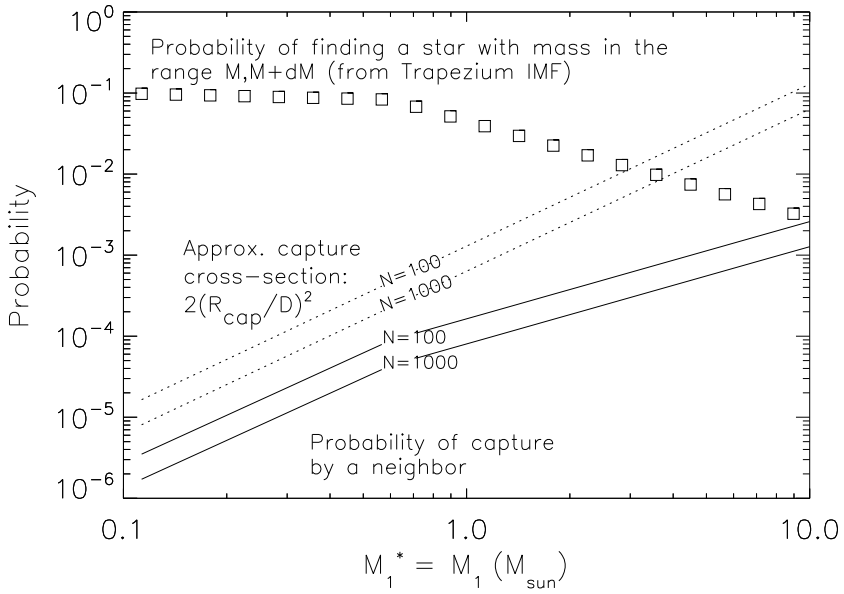

Fig. 7.— For a given source of remnants, the probability of capture by a neighbor of equal mass, shown in *solid* line, is given by $2(R_{cap}(m_1^*)/D)^2 \times (P_{IMF}(m_1^*))^{2/3}$; where $2(R_{cap}(m_1^*)/D)^2$ is shown in *dotted* line and $P_{IMF}(m_1^*)$ is the Trapezium IMF normalized to unity, shown as *square* symbols (Lada & Lada 2003).

5.4 Estimate of the Number of Weak Transfer Events

To calculate the total number of remnants that could get transferred between two neighboring planetary systems, the capture probability in §5.3 needs to be multiplied by the number of remnants, N_R, that a planetary system may eject before the cluster disperses. The main uncertainties in assessing whether weak transfer is a viable method for remnant transfer lie in estimating this number. Given the large uncertainties, in this sub-section (and the remainder of this paper) we will only estimate N_R for our Solar System, as it is the only planetary system for which observations and dynamical models enable us to make an educated estimate.

An estimate of N_R was given in Adams & Spergel (2005): assuming that the early solar nebula contained about 50–100 $M_\oplus$ of heavy elements, from which about one third was left-over from the planet formation process, and about one third of this left-over material was ejected from the planetary system during encounters with the giant planets, they estimated that during the time of planet formation, which lasted ~ 10 Myr, at least $M_R \sim 1$ $M_\oplus$ of

rocky material could have been ejected from a planetary system. Because clusters remain bound during 10–100 Myr, some of this rocky material could in principle get captured by other stars in the cluster. Of particular interst are the remnants ∼10 kg, large enough to shield any potential biological material from the hazards of radiation in deep space and from the impact on the surface of a terrestrial planet (Horneck 1993; Nicholson et al. 2000; Benardini et al. 2003; Melosh 2003).

5.4.1. Estimating N_R from the Oort Cloud

An estimate of N_R can be derived from observations and dynamical models of the Oort Cloud comets, which are weakly bound to the Solar System and are therefore representative of a population of remnants that may have been located on its weak stability boundary, subject to weak escape.

Oort Cloud formation scenario:
In a recent paper, Brasser, Duncan & Levison (2006) proposed the following scenario for Oort Cloud formation. Before the gas in the solar protoplanetary nebula dispersed, the gas giant planets Jupiter and Saturn formed, and subsequently scattered the Jupiter-Saturn zone planetesimals out to large distances. This process happened relatively quickly, before the Sun left its maternal stellar cluster and the cluster gas dispersed. At these distances, the planetesimals were subject to the gravitational perturbations of the cluster gas and stars; these perturbations cause a Kozai-like effect of coupled eccentricity–inclination oscillations. These long period oscillations in a slowly changing gravitational potential of the cluster, resulted in the lifting of the pericenter of the planetesimals' orbits beyond the orbit of Saturn. Close encounters with stars, in particular near the center of the cluster, also had the effect of increasing the pericenters. Planetesimals that achieved pericenters $\gg$ 10 AU were safe from complete ejection from the Solar System, and subsequently formed the Oort Cloud. (This model does not consider the ice giants Uranus and Neptune because they likely formed after the solar protoplanetary gas dispersed (>10 Myr), and probably after the Sun left the cluster.) Brasser et al. best estimate cluster model that correctly explains the current orbits of Sedna and 2000 CR_{105} and that makes Sedna a typical Oort Cloud member consists on a stellar cluster of 284 members, with a total mass in stars and gas of 419 $M_\odot$, a velocity dispersion of 1.755 km/s, a crossing time of 0.056 Myr, a Plummer radius of 0.1 pc and a tidal radius of the Sun of 0.013pc. In this model, 2–18% of the planetesimals in the Jupiter–Saturn region became part of the primordial Oort Cloud.

We adopt the above scenario to calculate N_R. First, we estimate the number of planetesimals in the Jupiter-Saturn zone, which we assume was the 4–12 AU heliocentric distance

zone; we assume that 2–18% of those ended up in the Oort Cloud.

Total mass of solids in the primordial 4-12 AU region:
To calculate how many planetesimals formed in this region, we estimate the total mass in solids (i.e. excluding H and He) that could have been available for the formation of planetesimals in the 4–12 AU region. We adopt the minimum mass solar nebula (MMSN), the minimum mass that the solar protoplanetary disk must have contained in order to form all the planets in the Solar System, given by the surface density $\Sigma = \Sigma_0(a/40AU)^{-3/2}$, where the surface density of dust (i.e. solids) has the coefficient $\Sigma_0 = \Sigma_{0d} = 0.1$ g/cm^2, (Weidenschilling 1977, Hayashi 1981). Integrating between 4 and 12 AU, we find the total mass in solids, 10^{29} g.

Planetesimal size distribution:
With the above estimate for the total mass in solids, we can calculate the number of planetesimals by adopting a planetesimal size distribution function representative of the early Solar System. This size distribution is highly uncertain, but can be constrained roughly from observations and coagulation models.

The current best observational estimate for the size distribution of outer Solar System planetesimals is for the trans-Neptunian Kuiper belt bodies studied by Bernstein et al. (2004). Theoretical estimates are based on planetesimal coagulation models, reviewed in Kenyon et al. (2007). Here we summarize these results, and use them to guide our estimates for N_R.

- Observations of Kuiper Belt bodies show, broadly, two dynamical classes, the Classical Kuiper Belt (CKB) with low inclination, low eccentricity orbits and the Excited Kuiper Belt (EKB) with moderate-to-high orbital inclinations and eccentricities. Bernstein et al. (2004) find that the size distribution functions of these two classes are different at a 96% confidence level. Each class is well fitted by a 'broken' power law, $dN/dD \propto \mathrm{D}^{-q_1}$ for $D > D_0$ and $\mathrm{dN/dD} \propto \mathrm{D}^{-q_2}$ if $\mathrm{D}<\mathrm{D}_0$, of different power law indices at the small and large sizes: $q_1^{CKB} \geq 5.85$ and $q_2^{CKB} \approx 2.9$ for the CKB, and $q_1^{EKB} \approx 4.3$ and $q_2^{EKB} \leq 2.8$ for the EKB. The break in the power laws is at $D_0 \approx 100$ km.

- The CKB has fewer large objects than the EKB; the maximum planetesimal size in the CKB is 60 times smaller than the maximum planetesimal size in the EKB. The EKB contains fewer small objects than the CKB. This differences indicate that the Excited population is likely "older – has undergone more collisional accretion and erosion – than the Classical population. This suggests that the EKB objects may have formed at smaller heliocentric distances than those in the CKB.

- For both populations, the size distribution of the small bodies is shallower than expected in a collisional cascade, $q_2 < 3.5$, where the latter value is a theoretical estimate for collisional cascades (Dohnanyi 1969). The break to a shallower size distribution occurs at $D \leq 100$ km, a size range susceptible to collisional destruction (Pan & Sari 2005). The observed strong depletion of the small bodies, and the fact that the collisional lifetimes in the present-day Kuiper belt are longer than the age of the Solar System, indicates that in the past both the CKB and EKB were more massive and richer in small bodies and that the present state is the result of an advanced erosional process.

- Theoretical models of planetesimal coagulation in the outer Solar System also find a broken power law size distribution function, with parameter values $q_1 \approx 2.7$–3.3 and $q_2 = 3.5$, and a break diameter $D_0 \approx 1$km (reviewed in Kenyon et al. 2007). These do not match the observations of the present-day Kuiper belt, but may be representative of its very early stage during the planet formation era.

Based on the above studies, we adopt three size distribution functions for our calculation of N_R.

- *Case A*: $q_1 = 4.3$, $q_2 = 3.5$, $D_0 = 100$ km, $\mathrm{D}_{max} = 2000$ km ($\sim$ Pluto's size), $\mathrm{D}_{min} = 1$ μm ($\sim$ dust blow-out size).
  This distribution has the power law index of a collisional cascade at the small size end, and that of the EKB at the large size end, with a break diameter consistent with that of the present-day Kuiper belt. The rough scenario this case reflects is as follows: In the Jupiter-Saturn zone, the accretion of large planetesimals proceeded to make the large-size end similar to that found in the present-day EKB, whereas at the small size end, the dynamical stirring by the large bodies produced a classical collisional cascade.

- *Cases B and C* $q_1 = 3.3$ and 2.7, $q_2 = 3.5$, $D_0 = 2$ km, $\mathrm{D}_{max} = 2000$ km ($\sim$ Pluto's size), $\mathrm{D}_{min} = 1$ μm ($\sim$ dust blow-out size):
  These size distributions are derived from theoretical coagulation models.

- *Case D*: $q_1 = 4.3$, $q_2 = 1.1$, $D_0 = 100$ km, $\mathrm{D}_{max} = 2000$ km ($\sim$ Pluto's size), $\mathrm{D}_{min} = 1$ μm ($\sim$ dust blow-out size):
  This size distribution represents perhaps the worst case scenario in which the depletion of the small bodies took place very early on, before the objects were thrown into the Oort Cloud. The parameters here are within the range that Bernstein et al. (2004) find for the EKB. This size distribution is also similar to that found in models for the primordial asteroid belt ($q_1 = 4.5$, $q_2 = 1.2$, $D_0 \sim 100$ km, Bottke et al. 2005).

Number of remnants with masses > 10 kg that could have been subject to weak escape: With the above estimates of the total mass in solids and of the size distributions, we can finally calculate the number of planetesimals with masses > 10 kg, equivalently, diameter $D > 26$ cm (assuming $\rho = 1$ g/cm^{-3}), that would have existed in the 4–12 AU region at the time of Jupiter and Saturn formation. The results are shown in Table 1. The scenario described in Brasser et al. (2006) finds that 2–18% of these planetesimals would have tranferred to the primordial Oort Cloud; these are also the bodies potentially available for weak escape from the early Solar System, hence they provide our estimate for N_R, also given in Table 1 for each of our cases. We find that N_R is in the range 10^{17}–$10^{20.5}$ for Cases A, B and C (which are based on a collisional cascade for the small objects), but is only 10^7–10^8 for Case D (which has a much shallower size distribution for the small bodies, similar to the observed Kuiper belt). It is clear that N_R is very sensitive to the size distribution function, i.e. power law index used.

5.4.2 Number of Weak Transfer Events in the Early Solar System

Now we estimate the number of weak transfer events from the early Solar System to the nearest solar-type star in the cluster (assuming it also harbored a planetary system) by multiplying N_R with the capture probability calculated in section 5.3 (see Fig. 5). For $M_1^* = M_1 = 1\ M_\odot$, the capture probability is 8.1×10^{-5} for N=1000 and 1.7×10^{-4} for N=100. The result is also listed in Table 1. The number of weak transfer events between two solar-type stars for Cases A, B and C are in the range $10^{13.1}$–$10^{16.7}$, and for Case D is 900–17000. As mentioned before, because the location of the renmant inside the weak stability boundary does not guarantee capture, these estimates should be regarded as upper limits.

5.5 Implications for Lithopanspermia

Because planetesimals could potentially harbor the chemical compounds that constitute the building blocks of life, it is of interest that the results above indicate that these materials could have been transferred in significant or even large quantities between the Solar System and other solar-type stars in its maternal cluster. For the case of binary systems, Adams & Spergel (2005) found that clusters of N = 30–1000 could experience billions to trillions of capture events among their binary members. However, to consider the transfer of microorganisms that developed in the Solar System, a necessary condition would be that life could develop during the 10–100 Myr that the cluster remained bounded. Radiometric measurements of hafnium and tungsten isotopes in meteorites indicate that the bulk of the metal-silicate separation in the Solar System occurred within the first 30 Myr of the solar nebula lifetime, with most of the Earth's core accreted during the first 10 Myr (Yin et al. 2002; Kleine et al. 2002). It is not known when the conditions for life to develop on Earth were met. There is evidence, albeit sparse, that basic habitable conditions (existence of continents and prevalance of liquid water) were established on Earth within $\sim$ 150 Myr of Solar System formation (e.g., Cates & Mojzsis 2007). The oldest Earth rocks are $\sim$ 3.9 Gyr old and some authors claim that the first traces of life appear just 100 Myr later (Mojzsis et al. 1996), but this result is controversial (Fedo & Whitehouse 2002). Similarly, there is controversy surrounding the finding of modern cyanobacteria in rocks 3.465 Gyr old (Schopf 1993; Brasier et al. 2002); undisputed is evidence of cyanobacteria and primitive eucaryotes in rocks 2.7 Gyr old (Brocks et al. 1999).

Transfer Timescales

For the transfer of microorganisms from the Solar System to other systems, we need to consider not only the timescale for life to develop, but also the timescale for weak transfer and how it compares to the timescale for microorganism survival in deep space.

- *Timescale for Ejection*: The time, T_R, for a remnant to exit the Solar System, i.e. to move from its periapsis (r_p) with respect to the central star to the distance $R_{esc}(m_1)$ can be is estimated using Barker's equation which yields the time of flight along a parabolic trajectory,

$$T_R = \frac{1}{2\sqrt{Gm_1}}(pL + \frac{1}{3}L^3),$$

where

$$L = \sqrt{p}\tan(\frac{\nu}{2}), \quad \nu = \arccos(\frac{p}{R_{esc}} - 1).$$

The variable ν is the true anomaly, and $p = 2r_p(= 2\Delta)$ is the semi-latus rectum. For $p \ll R_{esc}$ and using trigonometric identities it can be shown that L varies approximately independently from p : $L = \sqrt{2R_{esc}}\sqrt{1 - \frac{p}{2R_{esc}}} \approx \sqrt{2R_{esc}}$. Therefore, the variation of T_R as a function of r_p is negligible, so without loss of generality, we can examine the variation of T_R as a function of R_{esc} for a fixed periapsis distance of $r_p \approx 5$ AU: for stellar masses of 0.1 $M_\odot$, 1 $M_\odot$ and 10 $M_\odot$, Figure 4 shows that $R_{esc} = 1.8\times10^4$ AU, 1.8×10^5 AU and 1.8×10^6 AU, respectively, which yields $T_R \approx 0.6$, 6 and 60 Myr, respectively.

- *Timescale for interstellar transfer*: For a remnant moving at the low velocity of 0.1 km/s, as required by the weak transfer mechanism, it will take about 3.3–4.8 Myr to reach a neighboring star located at $D \approx 7\times10^4$–10^5 AU.

- *Timescale to land on a terrestrial planet*: Because it is not required that the captured remnant approaches the star in the ecliptic plane, multiple periapsis passages about the target star would be needed before the remnant can collide with a planet. This can take of the order of tens of millions of years.

- *Timescale for erosion from interplanetary dust*: In the interplanetary dust environment found in the Solar System, a meter-size rock will be ablated and eroded on a timescale of about 0.02–0.23 Myr, short compared to the time it takes to be ejected from the system (about 4 Myr; Napier 2004). It is likely that the early Solar System was significantly more dusty than it is today, thus survival times of remnants would have been even shorter, and much less than the several Myr transfer timescales.

Even if we were to assume that life arose on Earth before the stellar cluster dispersed, given the ejection and transfer timescales described above and the survival timescale of

dormant microoganisms, it seems unlikely that microorganisms could have been transferred even among the closest neighbors in the cluster via the weak transfer mechanism described here. However, our results that significant quantities of solid material could have been transferred via weak transfer between nearest neighbors in the Sun's birth cluster, are worth further investigation for the exchange of chemical compounds that constitute the building blocks of life and which could potentially have significantly longer survival lifetimes.

6. CONCLUSIONS

Could life on Earth have been transferred to other planetary systems within the first few Myr of the Solar System evolution, when the Sun was still embedded in its maternal aggregate?; and vice versa, could life on Earth have been originated beyond the boundaries of our Solar System?

In this paper we have described a dynamical mechanism that yields very low velocity chaotic escape of remnants from a planetary system using parabolic trajectories, and its reverse process of chaotic capture. These two processes provide a mechanism for minimal energy transfer of remnants between planetary systems. We have applied this mechanism to the problem of planetesimal transfer between planetary systems in an open star cluster, where the relative velocities between the stars are sufficiently low ($\sim$ 1 km/s) to allow slow escape and capture. Based on geometrical considerations, we have estimated upper limits to the probability of transfer that depend on the cluster properties and the masses of the source and target stars. Using these probabilities, adopting the Oort Cloud formation models from Brasser et al. (2006), and adopting a range of planetesimal size distributions derived from observations and theoretical models (Bernstein et al. 2004 and Kenyon et al. 2007, respectively), we estimate the number of weak transfer events from the early Solar System to the nearest solar-type star in the cluster (assuming it also harbored a planetary system). This estimate is most sensitive to the power law index of the size distribution of small bodies: the number of weak transfer events could be could be as large as $10^{13.1}$–$10^{16.7}$ if the size distribution of the small bodies follow a classical collisional cascade, or as small as 900–17000 if we adopt a shallower power law index for the size distribution of the small bodies. To determine whether the weak transfer process described in this paper could have been a viable mechanism for the transfer of remnants between the Solar System and other stars in the cluster, further progress needs to be made in the understanding of the dynamical and collisional history of the early Solar System.

Comets and asteroids have been suggested to be a possible source of the chemical compounds that constitute the building blocks of life on Earth. The results summarized above

are therefore of interest because they indicate that there is the possibility (depending on the shape of the size distribution) that planetesimal material could have been transferred via the weak transfer mechanism in large quantities between the Solar System and other stars in its maternal cluster.

Acknowledgments

E.B. acknowledges support from the NASA SMD/AISR program. A.M.M. is under contract with the Jet Propulsion Laboratory (JPL) funded by NASA through the Michelson Fellowship Program. JPL is managed for NASA by the California Institute of Technology. A.M.M. is also supported by the Lyman Spitzer Fellowship at Princeton University. R.M. acknowledges support from NASA's Outer Planets Program and from the Life and Planets Astrobiology Center (LaPLaCe) of the University of Arizona which is supported by the NASA Astrobiology Institute.

REFERENCES

Adams, F. C., & Spergel, D. N. 2005, Astrobiology, 5, 497

Adams, F. C., & Laughlin, G. 2004, Icarus, 150, 151

Belbruno, E. A., & Miller, J. 1990, Technical Report JPL IOM 312/90.4-1731-EAB

Belbruno, E. A., & Miller, J. 1993, J. Guid., Control and Dynamics, 16, 770

Belbruno, E. A., & Marsden, B. 1997, AJ, 113, 1433

Belbruno, E. A. 2004, Capture Dynamics and Chaotic Motions in Celestial Mechanics, (Princeton University Press)

Belbruno, E. A., & Gott III, J. R. 2005, AJ, 129, 1724

Belbruno, E. A. 2007a, Fly Me to the Moon: An Insider's Guide to the New Science of Space Travel (Princeton University Press)

Belbruno, E. A., Topputo, F., & Gidea, M. 2008, in Advances in Space Research, Vol. 42, 1330

Bernstein, G. M., Trilling, D. E., Allen, R. L., Brown, M. E., Holman, M., & Malhotra, R. 2004, AJ, 128, 1364

Binney, J., & Tremaine, S. 1988, Galactic Dynamics (Princeton University Press)

Brasser, R., Duncan, M. J., Levison, H. F. 2006, Icarus, 184, 59

Bottke, W. R., Durda, D. D., Nesvorny, D., Jedicke, R., Morbidelli, A., Vokrouhlicky D., & Levison, H. F. 2005, Icarus, 175, 111

Chambers, J. E. 2001, Icarus, 152, 205

Chazy, J. 1922, Annales Sci. de L'Ecole Norm. Sup., 3e Ser., 3, 22

Dones L. et al. 1999, Icarus, 142, 509

Easton, R. W. 1984, J. Diff. Equ. 52, 116

Garcia, R., & Gomez, G. Celestial Mechanics and Dynamical Astronomy, 2007, 97, 87

Gladman, B. 1997, Icarus, 130, 228

Gladman, B. et al. 1996, Science, 271, 1387

Hartmann, L. 2005, in ASP Conf. Ser. 271, Chrondrites and the Protoplanetary Disk, ed. A. N. Krot, E. R. D. Scott & B. Reipurth (San Francisco: ASP), 1003

Hayashi, C. 1981, Progress of Theoretical Physics Supplement, 70, 35

Horneck, G., Stöffler, D., Ott, S., Hornemann, U., Cockell, C. S. et al. 2008, Astrobiology, 8, 17

Keyon, S. J., Bomley, B. C., O'Brien, D. P., & Davis, D. R. 2008, in The Solar System Beyond Neptune, ed. A. Barucci, H. Boehnhardt, D. Cruikshank, & A. Morbidelli (Tucson: University of Arizona Press), 293

Kleine, T., Munker C., Mezger, K. Palme, H. 2002, Nature, 418, 952

Kummer, M. 1983, J. Math. Anal. Appl., 93, 142

Marsden, J., & Ross, S. 2006, Bull. Amer. Math. Soc., 43, 43

Melosh, H. J. 2003, Astrobiology, 3, 207

Melosh, H. J., Tonks, W. B. 1994, Meteoritics, 28, 398

Moro-Martín, A., & Malhotra, R. 2003, AJ, 125, 2255

Moro-Martín, A., & Malhotra, R. 2005, ApJ, 633, 1149

Moser, J. 1973, Stable and Random Motions in Dynamical Systems, Annals of Mathematics, Vol. 77 (Princeton University Press).

Racca, G. 2006, Celestial Mechanics and Dynamical Astronomy, 85, 1

Sitnikov, K. A. 1960, Dokl. Akad. Nauk USSR, 133, 303

Stöffler, D., Horneck, G., Ott, S., Hornemann, U., Cockell, C. S. et al. 2007, Icarus, 186, 585

Weidenschilling, S. J. 1977, Astrophys. Space Sci., 51, 153

Xia, Z. 1992, JDE, 96, 170

Yin, Q., Jacobsen, S. B., Yamashita, K., Blichert-Toft, J., Telouk, P. & Albarede, F. 2002, Nature, 418, 949

Table 1. Estimated Number of Weak Transfer Events

Planetesimal Size Distribution[a]	$N_{D>26cm}$[b]	N_R[c]	N_{WTE}[d] (N=100)	N_{WTE}[d] (N=1000)
A: $q_1 = 4.3$, $q_2 = 3.5$ $D_0 = 100$ km	1.8×10^{21}	3.6×10^{19}-3.2×10^{20}	6.1×10^{15}-5.5×10^{16}	2.9×10^{15}-2.6×10^{16}
B: $q_1 = 3.3$, $q_2 = 3.5$ $D_0 = 2$ km	2.7×10^{20}	5.4×10^{18}-4.9×10^{19}	9.2×10^{14}-8.3×10^{15}	4.4×10^{14}-3.9×10^{15}
C: $q_1 = 2.7$, $q_2 = 3.5$ $D_0 = 2$ km	8.1×10^{18}	1.6×10^{17}-1.4×10^{18}	2.7×10^{13}-2.5×10^{14}	1.3×10^{13}-1.2×10^{14}
D: $q_1 = 4.3$, $q_2 = 1.1$ $D_0 = 100$ km	5.5×10^{8}	1.1×10^{7}-9.9×10^{7}	1.9×10^{3}-1.7×10^{4}	8.9×10^{2}-8.0×10^{3}

[a]For all the

[b]$N_{D>26cm}$ is
> 10 kg if $\rho =$

[c]N_R is the
primordial Oo

[d]N_{WTE} is th
and N=1000
1.7×10^{-4} for